CHEMICAL ENGINEERING TRANSACTIONS
VOL. 62, 2017
A publication of AIDIC
The Italian Association of Chemical Engineering
Online at www.aidic.it/cet
Guest Editors: Fei Song,Haibo Wang, Fang He

ISBN978-88-95608- 60-0; **ISSN** 2283-9216
DOI: 10.3303/CET1762063

Hydrodynamics and Heat Transfer of Turbulent Flow around a Rhombus Cylinder

Suvanjan Bhattacharyya[*a], Asif Iqbal Khan[a], Deb Kumar Maity[a], Saikat Pradhan[a], Anshuman Bera[b]

[a]Department of Mechanical Engineering, MCKV Institute of Engineering, Liluah. Howrah, West Bengal. India.
[b]Department of Mechanical Engineering, Budge Budge Institute of Technology, Nischintapur. West Bengal. India.
suvanjanr@gmail.com

Three dimensional turbulent channel flow and heat transfer in the presence of a rhombus cylinder were studied numerically. The Reynolds number ranges from 100–20,000. Air has been used as a working fluid. In this paper, transition - SST model has been applied for numerical simulations. The Computation was made for four channel blockage ratios at different Reynolds. The wall boundary layer of the channel starts detached when a rhombus cylinder is placed in the channel, and a later swirling zone appears behind the cylinder. The results indicate that in presence of rhombus cylinder, heat transfer in the channel is augmented significantly. Nusselt number and friction loss increased with increase of blockage ratio. Numerical results indicate that the use of rhombus cylinder, the channel can increase the heat transfer performance.

1. Introduction

In the present scenario in many industrial applications turbulent flow (Rahimi et al., 2017) within the systems is being observed. The theoretical and practical significance of flow around cylinders of circular shape is most essential in the field of thermal engineering and fluid mechanics and are studied precisely. Bluff bodies which are cylindrical structures that are found in group or individually in designing of heat exchangers for locomotive, cooling system for nuclear power plants, buildings, chimneys, power lines, offshore structures, grids, screens, and cables, in both air and water as the flowing medium. Flow around cylinders precisely shows several essential phenomenon of physical importance which is separation of flow, vortex shedding and laminar to turbulent shifting of flow. Form of flow, energy transformation and flow characteristics are strictly guided by the shape of the bluff bodies. The efficiency of flow or heat exchanger can be deviated and reduced from the desired values depending upon the correct shape and dimension of the bluff bodies. Thus in designing of bluff cylinders the determination the shape and dimensions of the bluff cylinders are of much importance.

The prime motive of researchers is to save the energy as well as the costing also. In this way researchers find amplification of transfer of heat as a very significant matter to look upon. Strengthening of transfer of heat in channels such as in process industries or in engineering systems is relevant in designing of heat exchangers. Insertion of geometrical structures like vortex generators in the form of delta wing, spring tape or ribs has been already applied for the appreciation of heat transfer. The most primitive conformation of a bluff body is an element of prism like structure for this it is not studied specifically whereas flow around cylinders and square cylinders have been studied precisely as they are practically relevant in use. Abbasi et al., (2002) showed for enhancement of transfer of heat in a channel use of prism could be gainful. But the FEM analysis is confined to laminar regime only. Experimental observation showed that around Re=100, triangular prism can be used for effective enhancement of transfer of heat. Presence of vortex generators in flow field results in longitudinal vortices that includes mixing which in turn enhances heat transfer (Elyyan et al., 2010; Park et al., 1998; Benim et al., 2011). A substantial amount of transfer of heat was recognized when the flow field became periodic. Jackson (1987) investigated using finite element simulation how the occurrence of bodies with dissimilar shapes effect the transfer of heat rate. In complex analysis introduction of CFD contributes vastly in the investigation of the flow field that minimizes the effort and ranged it within desktop computers. Direct estimation of transport variables can be done readily but it has to be confirmed considering each and every

Please cite this article as: Suvanjan Bhattacharyya, Asif Iqbal Khan, Deb kumar Maity, Saikat Pradhan, Anshuman Bera, 2017, Hydrodynamics and heat transfer of turbulent flow around a rhombus cylinder, Chemical Engineering Transactions, 62, 373-378
DOI:10.3303/CET1762063

aspect. Dhiman et al., (2015) investigated steady and unsteady forced convection flow and heat transfer past over a semi-circular bluff body for the air as working fluid for Re=1–40. Rashidi et al., (2015) investigated heat transfer of a nano fluid over equilateral triangle obstacle. Dhinakaran (2011) investigated heat transfer from a bluff body (cylinder) near a moving wall at Re=100. Moinat et al., (2000) studied the turbulent separated-reattaching flow region over a bluff rectangular plate using the large-eddy simulation (LES) technique and with three sub grid-scale models. Reynolds number is taken as 50,000 and blockage ratio of 5.6%.
In the present work, numerical analysis of turbulent flow and heat transfer in a 3-D channel with rhombus cylinder (RC) located inside was performed. The different blockage ratio of the RC is investigated. While the channel length was 30D, the position of the bluff cylinder (RC) was sustained at X=15D. This arrangement was closer to the geometry of Chattopadhyay (2007) which was used as a benchmark.

2. Problem Formulation and Governing Equation

The present computational analysis reflects the forced convection cross flow around a bluff body (RC), as shown in Figure 1. The hydraulic diameter of the channel is D. The non-dimensional space between the inlet of the channel and the surface of the bluff cylinder (RC) is 15D with the total non-dimensional length of the computational domain is 30D. The non-dimensional blockage ratio is the height of the cylinder to the hydraulic diameter of the channel, (Ƀ =0.8, 0.7, 0.6, 0.5 and 0.4) has been used in this work. The problem is considered to be three-dimensional. Air (Pr 0.71) is considered as working fluid.

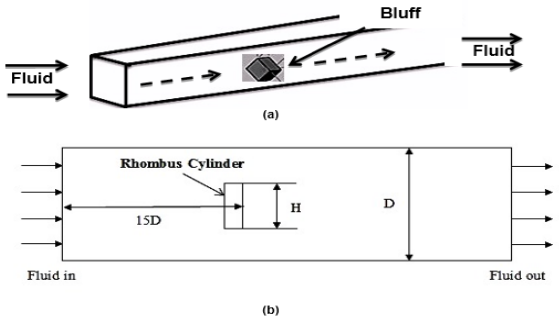

Figure 1: (a) Layout of the channal containing Rhombus Cylinder, and (b) Computational domain

Steady-state, incompressible flow of a Newtonian fluid with constant properties is investigated. Body forces, viscous dissipation and radiative heat transfer are neglected. Turbulence is modelled within a RANS (Reynolds Averaged Numerical Simulations) approach. For the computational analysis, the finite volume method based general purpose CFD software ANSYS Fluent 16.2 is employed (www.anysy.com). As turbulence model, the transition SST model of Menter et al., (2002) is employed, which was recently used by Kadiayala et al., (2017) for studying the effects of jets on moving surface and by Bhattacharyya et al., (2017) in studying heat transfer enhancement. The model is proficient of effortlessly bridging laminar and turbulent regimes. For both flow regimes, a fluctuation turbulent intensity at the inlet can be prescribed. Abraham et al. (2009) employed this procedure for fluid flow through pipe in laminar and turbulent regimes and seen outstanding agreement at all ranges.
The Reynolds averaged governing equations are summarized below (overbars that are normally used to indicate Reynolds averaged quantities are omitted, for simplicity).

$$\frac{\partial u_i}{\partial x_i} = 0,\ i = 1, 2, 3 \tag{1}$$

$$\rho\left(u_i \frac{\partial u_j}{\partial x_i}\right) = -\frac{\partial p}{\partial x_i} + \frac{\partial}{\partial x_i}\left((\mu + \mu_{turb})\frac{\partial u_i}{\partial x_i}\right),\ j = 1, 2, 3 \tag{2}$$

$$(\mu_i \frac{\partial \Theta}{\partial u_i}) = \frac{\partial}{\partial x_i}((\alpha + \frac{\upsilon_{turb}}{Pr_{turb}})\frac{\partial \Theta}{\partial x_i}) \tag{3}$$

The term Pr_t is function of Re .The turbulent closure as already discussed is using the SST model of Menter et al. (2002) where ω is the specific rate of the turbulence kinetic energy k, and the terms α_k , α_ω and $\alpha_{\omega 2}$ are Prandtl number-like parameters for the transport k, ω. Furthermore, F_1, F_2 is a blending function that simplifies the grouping of the standard k-ϵ model. The term S is the absolute value of the shear strain rate and the β terms are model constant.

$$\frac{\partial(\rho\mu_i k)}{\partial x_i} = \gamma P_k - \beta_1 \rho\kappa\omega + \frac{\partial}{\partial x_i}[(\mu + \frac{\mu_{turb}}{\sigma_k})\frac{\partial k}{\partial x_i}] \tag{4}$$

$$\frac{\partial(\rho\mu_i \omega)}{\partial x_i} = A\rho S^2 - \beta_2 \rho\omega^2 + \frac{\partial}{\partial x_i}\left[\left(\mu + \frac{\mu_{turb}}{\sigma_\omega}\right)\frac{\partial \omega}{\partial x_i}\right] + 2(1 - F_1)\rho\frac{1}{\sigma\omega_2 \omega}\frac{\partial k}{\partial x_i}\frac{\partial \omega}{\partial x_i} \tag{5}$$

Where, $\mu_{\text{turb}} = \frac{\alpha\rho\kappa}{\max(\alpha\omega,\text{SF}_2)}$

The intermittency factor γ, which multiplies the production term P_k in ranges between 0 and 1.Thus it can diminish the turbulence product up to zero level in laminar regime .Additional equations are needed to solve γ, as this term is also coupled with a new variable which described the local stability status of the flow in the near-wall region.

The working equations for the intermittency and intermittency adjunct function Π adopted Menter et al. (2002) and Abraham et al. (2009) are given below.

$$\frac{\partial(\rho\gamma)}{(\partial t)} + \frac{\partial(\rho u_i\gamma)}{\partial x_i} = P_{\gamma,1} - E_{\gamma,1} + P_{\gamma,2} - E_{\gamma,2} + \frac{\partial}{\partial x_i}\left[\left(\mu + \frac{\mu_{turb}}{\sigma_\gamma}\right)\frac{\partial\gamma}{\partial x_i}\right] \quad (6)$$

$$\frac{\partial(\rho\pi)}{\partial t} + \frac{\partial(\rho u_i\pi)}{\partial x_i} = P_{\pi,t} + \frac{\partial}{\partial x_i}\left[\sigma_{\pi,t}(\mu + \mu_{turb})\frac{\partial\pi}{\partial x_i}\right] \quad (7)$$

3. Boundary conditions and solution procedure

The inlet velocity of the fluid of U_∞ and temperature of the inlet fluid is $T_\infty$where the channel wall constant surface temperature is maintained about T_s =398 K. The fluid is defined to be air with constant physical properties (Pr=0.71) with an inlet temperature of 298 K. Following Abraham et al. (2009), for the inlet turbulence intensity, 5% was assumed for all cases.

Table 1. Grid independence study

	Total number of grid nodes	Nu	f	η
Grid 1	798,777	44.423461	0.0492391	1.323929
Grid 2	970,000	44.496366	0.0497496	1.338917
Grid 3	991,852	44.499351	0.0499112	1.339012

The governing equations were solved using commercial CFD software ANSYS fluent 16.2 (www.anysy.com). The momentum equation was discretized with second order accurate upwinding scheme for attaining desired level of precision and the energy equation was solved using third-order MUSCL Van Leer (1979). The convergence criteria for continuity, momentum and energy were set at 10^{-5}, 10^{-5}, and 10^{-7} respectively. The convergence criteria for the turbulence quantities were fixed at 10^{-4}.

After performing rigorous check for grid independence, adequate numbers of cells were used. The numbers of cells for the rhombus cylinder a mesh with 970,000 cells were used. It was found that further refinement of grids do not lead appreciable change in results such Nusselt number and performance evaluation criteria (PEC) distribution. In proceeding section, validation with correlations and available data from literature is also discussed. For ensuring sufficiently low discretization errors, a grid independence study was performed (for the case with Ƀ =0.8 and Re=10,000), the results of which are shown in Table 1.

4. Results and discussion

Parameters and Correlations Used in Evaluating the Results

The Reynolds number of air flow in the duct is calculated from,

$$Re = \frac{v \times D}{\nu} = \frac{\rho \times v \times D}{\mu} \quad (8)$$

The convective heat transfer coefficient is then used to obtain Nusselt number, Nu, as,

$$Nu = \frac{h \times D}{K} \quad (9)$$

The friction factor is determined from the measured values of pressure drop (ΔP), across the test section length.

$$f = \frac{2 \times \Delta P \times D}{4 \times \rho \times L \times V^2} \quad (10)$$

To evaluate the effect of heat transfer enhancement under given pumping power, the performance evaluation criteria (η) is employed by Bhattacharyya et al. (2017),

$$\eta = \frac{Nu}{Nu_0} \Big/ \frac{f}{f_0}^{0.33} \quad (11)$$

Where Nu and Nu_0 are Nusselt numbers for the enhanced channel and the plain channel respectively, f and f_0 are friction coefficients for enhanced channel and plain channel respectively.

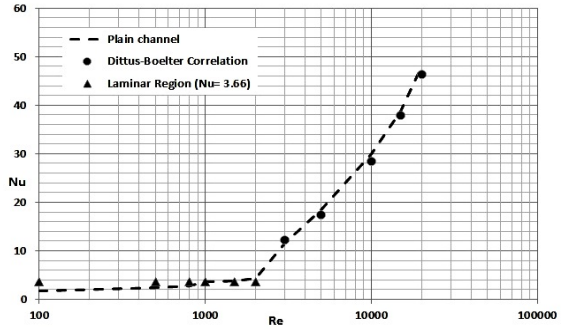

Figure 2: Comparisons of simulation data and correlations of the plain channel for Nusselt number

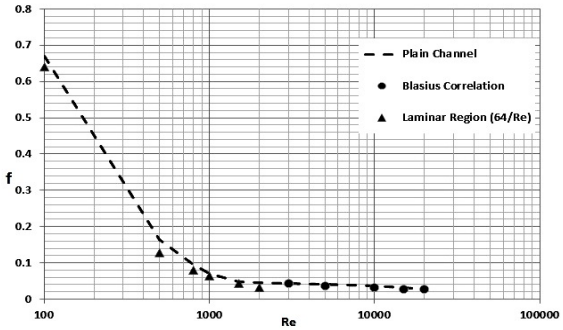

Figure 3: Comparisons of simulation data and correlations of the plain channel for friction factor

For fully developed laminar flow in plain channel with isothermal walls, analytical expressions exist for the friction factor and the Nusselt number that state (Ozisik 1985):

$$f=64/Re \quad (12)$$

$$Nu=3.66 \quad (13)$$

For fully developed turbulent flow in a channel with plain walls, among others, the following correlations exist for the friction coefficient (f) and the Nusselt number (Nu):

Blasius correlation (Ozisik 1985)

$$f = 0.3164\ Re^{-0.25} \quad (14)$$

Dittus-Boelter correlation (Ozisik 1985):

$$Nu = 0.023\ (Re)^{0.8} \times (Pr)^{0.33} \quad (15)$$

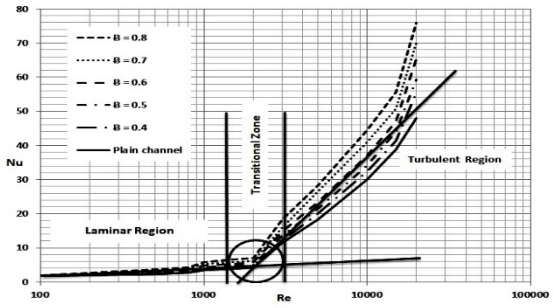

Figure 4: Variation of Nusselt number with Reynolds number for different blockage ratio of RC

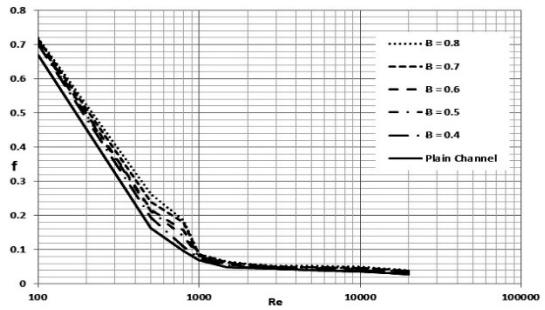

Figure 5: Variation of friction factor with Reynolds number for different blockage ratio of RC

Results of the Plain channel

The numerical results on heat transfer and pressure drop characteristic in terms of Nusselt number and friction factor of the plain channel are presented and validated with the above correlations. From Figure 2 and Figure 3 one can see that the results from the plain channel agree well with those from the standard correlations within ± 3% deviations for Nusselt number and ±5% for friction factor.

The numerical results of heat transfer characteristics under a constant wall temperature with bluff cylinders (RC) inserts of different blockage ratio are reported in the Figure 4. The Reynolds number ranges from 100 – 20,000. It is clear from the figure that SST model can work throughout the all flow regime. As proposed by Abraham et al. [20], prediction of transition from laminar to turbulent regime is done. By drawing tangents at the laminar data ranges and at the end turbulent regime, we can recognize the transition zone in the figure. As such, the slope of Nu –Re plot is different for laminar and turbulent zones. It is observable that the transition zone falls around Re 3000-4000. Nu significantly increases with the rise of Reynolds number, replicating that the increase of convective heat transfer. Obviously, all RC give improved heat transfer improvement in terms of Nusselt numbers, than the plain channel. The greater Nu of RC can be recognized to their mixing effect,

recirculation zone and vortex generation. Among the different blockage ratio, the RC with blockage ratio (Ƀ =0.8) shows the highest heat transfer. This specifies that the Nu increases with increase of blockage ratio.
Results of all studied RC of pressure drop in the form of friction factor characteristic is shown in Figure 5. The figure shows that the relationship between the friction factor and Reynolds number at different blockage ratios (Ƀ=0.8, 0.7, 0.6, 0.5 and 0.4) for all channel fitted with RC and plain channel. The friction factor outcomes are opposed to the Nusselt number results. For all the cases, friction factor conventionally decreases with the increasing Reynolds number. It could be also seen from the figure that the friction factor was in the similar trend both for the channel with RC and the plain channel. The friction factor increases with the increase of blockage ratio. This is because the attributed to the use of RC with a higher blockage ratio which led to a higher viscous loss near the tube wall regions caused by a stronger vortex generation or mixing flow and long residence time in the channel.

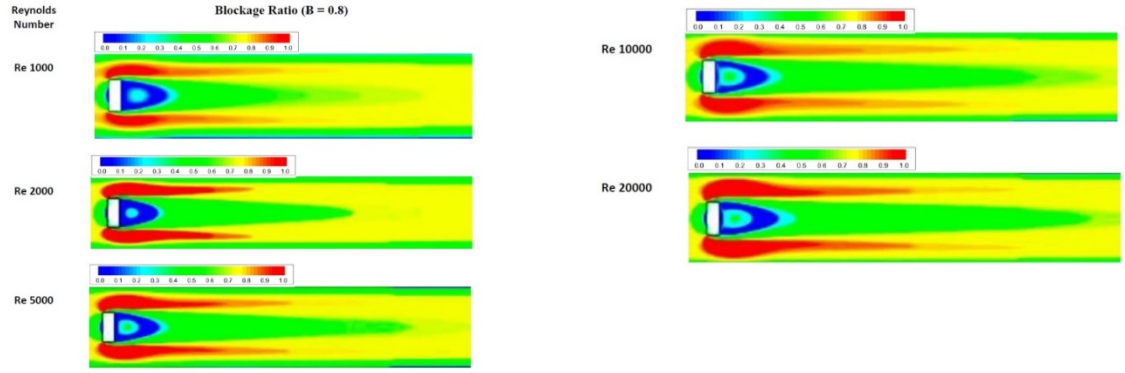

Figure 6: Dimensionless velocity contour plots around RC for Ƀ =0.8 at different Reynolds number

Results for the channel with RC

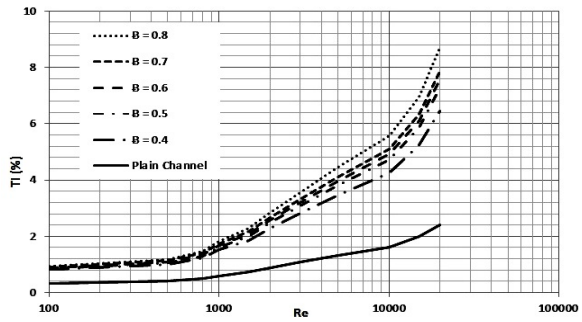

Figure 7: Variation of turbulent intensity (TI in percentage) with Reynolds number for different blockage ratio of RC

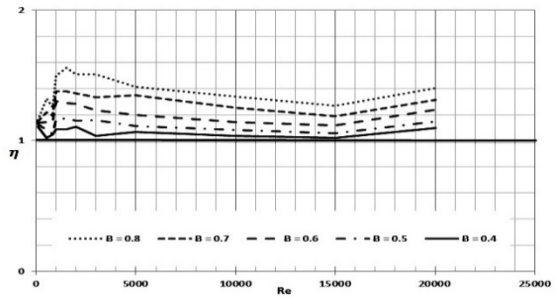

Figure 8: Variation of enhancement efficiency with Reynolds number for different blockage ratio of RC

To explain the differences in results caused by the RC, taken Re 1000, 2000, 5000, 10000, and 20000 as an example and present the plots of axial-velocity contours as shown in Figure 6.
Figure 6 displays detail view of dimensionless velocity ((u=U/u*)) through a horizontal slice of the channel with blockage ratio (Ƀ=0.8). It can be observed that Ƀ has strong influence over the flow field as higher blockage ratio leads to reduced flow strength. By considering the figures, one can notice that the flow fields are almost similar for all the cases. Turbulent Intensity at the outlet of the channel is shown in Figure 7. Turbulent dies out for low Reynolds number (Re = 100) and rises with increasing Reynolds number. At the entrance of the channel, 5% turbulent intensity (TI) is enforced following Abraham et al. [21]. From the figure, one can see that the highest level of turbulent intensity is about 7.5% - 8.6% at Re of 15,000 - 20,000.As augmentation in heat transfer is gradually accompanied by pressure drop, thermal performance factor (η) is the correct parameter used for assessing the practical use of RC. The factor is found by considering the effect of heat transfer augmentation and the increase of friction penalty, simultaneously. The variation of η with Reynolds number of the channel equipped with RC is shown in Figure 8. By doing all the simulation on RC at different blockage ratio it was found effective from the energy point of view and augmentation efficiency was found to be greater

than the unity at most of the time in varied Reynolds number. The augmentation efficiency above unity directed that the outcome of heat transfer improvement due to RC was more dominant than the effect of rising friction and vice versa. As likely the channel with RC of blockage ratio (B = 0.8) provided higher thermal enhancement efficiency than the other tested blockage ratio.

5. Conclusion

Numerical analyses have been conducted to study the effect of heat transfer and flow characteristics around a rhombus cylinder. The order of augmentation is about 30% - 31% as compared to plain channel. Nevertheless, as estimated, the enhancement is related with enhanced skin friction. The effect of aspect ratio of the RC, 3-D of the flow field and density variation are some of the significant features, which were not spoken in the present study and is planned to be studied in future. The thermal enhancement efficiency for all the cases was more than unity, shown that the outcome of heat transfer augmentation due to RC was more dominant than the effect of rising friction.

Reference

Abbassi H., Turki. S., Nasrallah. S.B., 2002, Numerical investigation of forced convection in a horizontal channel with a built-in triangular prism. ASME J. Heat Transfer, 124, 571–573.

Abraham J.P., Sparrow E.M., Tong J.C.K., 2009, Heat Transfer in All Pipe Flow Regimes: Laminar, Transitional/Intermittent, and Turbulent. International Journal of Heat and Mass Transfer, 52, 557–563.

Benim A.C., Chattopadhyay H., Nahavandi A., 2011, Computational Analysis of Turbulent Forced Convection in a Duct with a Triangular Prism. International Journal of Thermal Sciences, 50, 1973-1983.

Bhattacharyya S., Chattopadhyay H., Benim A.C., 2017, Simulation of Heat Transfer Enhancement in Duct Flow with Twisted Tape Insert. Progress in Computational Fluid Dynamics, an International Journal, 17(3), 193-197.

Bhattacharyya S., Chattopadhyay H., Haldar A., 2017, Design of twisted tape turbulator at different entrance angle for heat transfer enhancement in a solar heater. Beni-Suef Univ. J. Basic Appl. Sci. (Online published), DOI: 10.1016/j.bjbas.2017.08.003.

Chattopadhyay H., 2007, Augmentation of Heat Transfer in a Duct using a Triangular Prism. International Journal of Thermal Sciences, 46, 501–505.

Dhinakaran S., 2011, Heat transport from a bluff body near a moving wall at Re=100. International Journal of Heat and Mass Transfer, 54, 5444 - 5458.

Elyyan M.A., Tafti D.K., 2010, Effect of Coriolis Forces in a Rotating Duct with Dimples and Protrusions. J. Heat Fluid Flow, 31, 1–18.

Jackson C.P., 1987, A finite element study of the onset of vortex shedding in flow past variously shaped bodies. J. Fluid Mech, 365, 23–45.

Kumar A., Dhiman A., 2015, Laminar Flow and Heat Transfer Phenomena Across a Confined Semicircular Bluff Body at Low Reynolds Numbers. Heat Transfer Engineering, 36(18), 1540-1551.

Menter F., Esch T., Kubacki S., 2002, Transition modelling based on local variables. Proceedings of the Fifth International Symposium on Engineering Turbulence Modelling and Measurements, Mallorca, Spain.

Ozisik M.N., 1985, Heat Transfer: A Basic Approach. Mc-Graw-Hill, New York, USA.

Park J., Kwon K., Choi H., 1998, Numerical solutions of flow past a circular cylinder at Reynolds number up to 160. KSME Int. J., 12, 1200-1205.

Rahimi M., Soran R.A.., 2017, Numerical Analysis of Heat Transfer and Flow Field Due to Slot Air Jet Impingement for the Cases of Moving Plate and Moving Nozzle. Iran J. Sci. Technol Trans Mech Eng. 41, 217.

Rashidi S., Bovand M., Abolfazli Esfahani J., 2015, Structural optimization of nanofluid flow around an equilateral triangular obstacle. Energy (online Published), DOI: 10.1016/j.energy.2015.05.056: 1-14.

Suksangpanomrung A., Djilali N., Moinat P., 2000, Large-eddy simulation of separated flow over a bluff rectangular plate. International Journal of Heat and Fluid Flow, 21, 655 – 663.

Van Leer B., 1979, Towards the ultimate conservative deference scheme. V. A second-order sequel to Godunoy's method. J. Computational Physics, 32, 101-136.